A Cloud Strip as a Streamline of Radioactivity Radon and Epicenter Prediction by Electric Field Measurement

Fumitaka Inuyama   Senior Power Engineer (e-mail: inusanin@yahoo.co.jp)

Permanent address: 5-17-33 Torikai Jonan-ku, Fukuoka City, 814-0103, Japan

Thermal Power Dept., Kyushu Electric Power Co., Inc.(www.kyuden.co.jp) (Retired)

Abstract

Underground solid matter emits ground current, sound wave, light, electromagnetic wave, ion, radon, salts, groundwater, etc. as a process leading to destruction. In particular, an abnormal increase in the concentration of radon in the atmosphere has been observed as a presage of an earthquake in the Hyogo South Earthquake in 1995. A large amount of radon released from the ground continuously in time moves along the path while emitting radiation, and nitrogen, oxygen, and water in the atmosphere are ionized one after another, become continuous condensation nuclei, collect the surrounding moisture, and form a single cloud below the dew point temperature. The streamline of radioactivity radon is calculated by Newton's equation of motion as a single-article cloud grain. Therefore, if a cloud strip can be observed as a presage of an earthquake, the epicenter can be identified.

In addition, the epicenter can be predicted by observing the change in the underground electric field due to the charge near the epicenter caused by the contact triboelectric charge of rocks at seven points.

1. Streamline of Radioactivity Radon

1. 1 . The Process of Generating Clouds

When different substances A and B are contacted and pressed, a clear variation in the charge and electric field of the test sample surface is observed in the compression destruction of the rock so that the electron moves toward one substance due to the friction and positive and negative static electricity is charged. However, since the Earth's crust is negatively charged, the ⊖ charge locally stays in the crust. The ⊖ charge in the crust attracts the ⊕ charge moisture in the atmosphere by a weak coulomb force.

In addition, solid crust matter emits ground current, sound wave, light, electromagnetic wave, ion, radon (Fig.1), salts, groundwater, etc. as a process leading to destruction.

Measurements at Kobe Pharm. Univ. 25 km from the epicenter of the M7.3 Hyogo South Earthquake that occurred on January 17, 1995.[1]
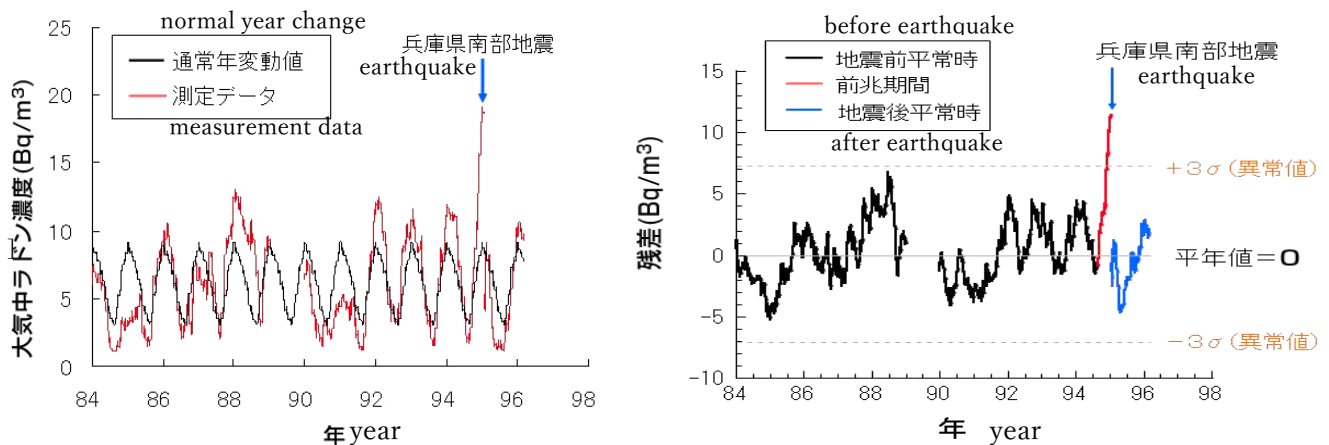

Fig.1 Changes in atmospheric radon concentration before and after earthquakes

A large amount of radon released from the ground continuously in time moves along the path while emitting radiation, and nitrogen, oxygen and water in the atmosphere are ionized one after another as shown in Fig. 2. It becomes continuous cloud condensation nuclei, collects the surrounding moisture, and forms a cloud below the dew point temperature. This is the same phenomenon in the cloud chamber that examines the traces of cosmic rays [2] .

Fig.2 Occurrence in the cloud chamber
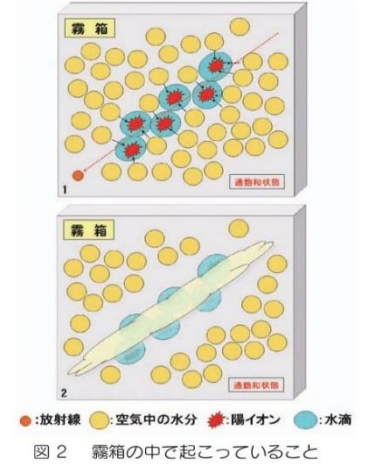
1. 2. The Basic Equations of Radon Flow

As a calculation model, it is considered that the vertical z axis stands on atmosphere ground boundary layer about 100 meters above the earth surface, and the horizontal x-axis is downwind direction in the x-y face and that wind velocity $(V_x, 0, V_z)$ And the earthquake focal depth d_o, the charge Q of the crust, the charge q of the cloud. It also takes into account with Stokes' viscous resistance and gravity. The basic equation of radon flow is as follows.

$$m\frac{d^2x}{dt^2} + 6\pi\mu r\left(\frac{dx}{dt} - V_x\right) + \frac{Qq}{4\pi\varepsilon_o\varepsilon_r}\cdot\frac{\partial}{\partial x}\left[\frac{-1}{\sqrt{x^2+y^2+(z+d_o)^2}}\right] = 0$$

$$m\frac{d^2y}{dt^2} + 6\pi\mu r\left(\frac{dy}{dt}\right) + \frac{Qq}{4\pi\varepsilon_o\varepsilon_r}\cdot\frac{\partial}{\partial y}\left[\frac{-1}{\sqrt{x^2+y^2+(z+d_o)^2}}\right] = 0$$

$$m\frac{d^2z}{dt^2} + 6\pi\mu r\left(\frac{dz}{dt} - V_z\right) + \left(m - \frac{4\pi r^3\rho}{3}\right)g + \frac{Qq}{4\pi\varepsilon_o\varepsilon_r}\cdot\frac{\partial}{\partial z}\left[\frac{-1}{\sqrt{x^2+y^2+(z+d_o)^2}}\right] = 0$$

From here, the description of the symbol is simplified as follows.

$$C(z) = 6\pi\mu r\,, \quad Q^{'} = \frac{Qq}{4\pi\varepsilon_o\varepsilon_r}, \quad G(z) = \left(m - \frac{4\pi r^3\rho}{3}\right)g\,, \quad \sqrt{} = \left[\frac{-1}{\sqrt{x^2+y^2+(z+d_o)^2}}\right]$$

$$m\frac{d^2x}{dt^2} + C(z)\left(\frac{dx}{dt} - V_x\right) + Q'\cdot\frac{\partial\sqrt{}}{\partial x} = 0$$

$$m\frac{d^2y}{dt^2} + C(z)\left(\frac{dy}{dt}\right) + Q'\cdot\frac{\partial\sqrt{}}{\partial y} = 0$$

$$m\frac{d^2z}{dt^2} + C(z)\left(\frac{dz}{dt} - V_z\right) + G(z)g + Q'\cdot\frac{\partial\sqrt{}}{\partial z} = 0$$

1. 3. The Solution of the Radon Flow Equations

As the numerical magnitude of each term of the basic equation, the charge term $Q' \sim 10^{-20}$ is very small compared to the viscous terms $C(z) \sim 10^{-9,}$ the wind velocity terms $mV_z \sim 10^{-13}$, and the gravity term $G(z)$ $\sim 10^{-12,}$ so it can be Q' omitted. PC numerical analysis of differential equations also prevents charged cloud grains from approaching less than a few percent the epicenter by coulomb forces. As a result, the basic equations can be simplified. Since air density ρ is a function of altitude z, it is a primary approximation of the viscous term $C(z)$, the gravity term $G(z)$. The same is possible with wind velocity. (Fig.3, Fig.4)

$$C(z) = -az + b \qquad G(z) = \alpha z + \beta \qquad (\ a, b, \alpha, \beta > 0\ ) \qquad z < 10{,}000 \ \text{m}、$$

$$V_x(z) = \varepsilon z + V_{x0} \qquad V_z(z) = -\eta z + V_{z0} \qquad (\ \varepsilon, \eta > 0\ ) \qquad \text{[Appendix 2]}$$
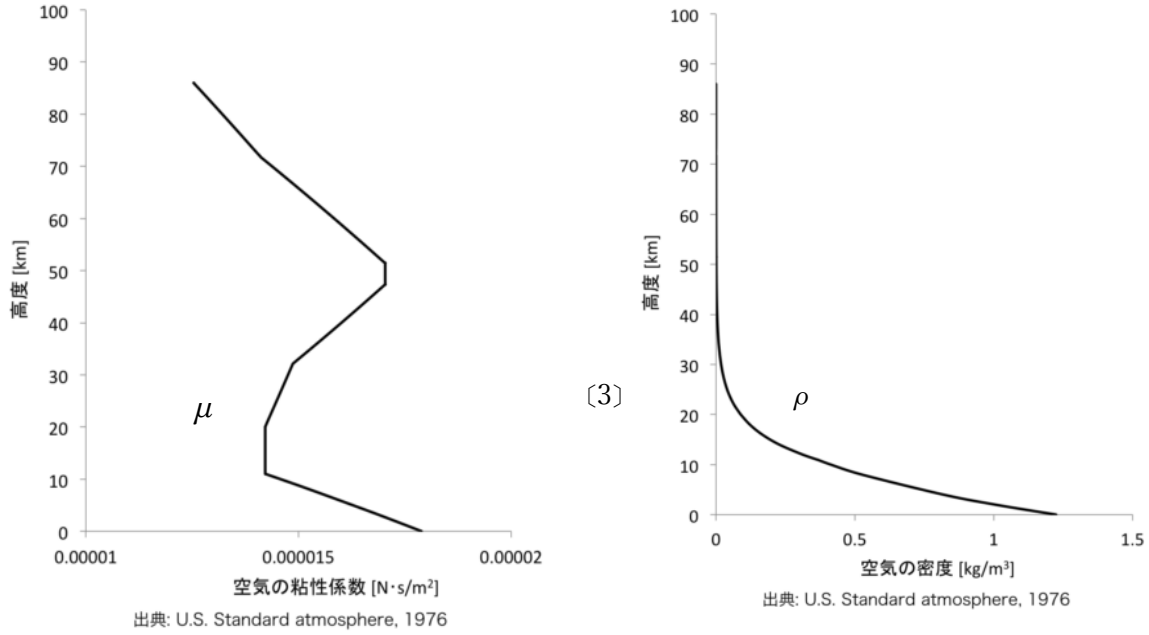

出典: U.S. Standard atmosphere, 1976

出典: U.S. Standard atmosphere, 1976

Fig. 3 Viscosity μ and density ρ of air vs altitude

To analyze basic equations in primary mathematics
dx/dt coefficients for C must be a constant, $C(z)=C_0$.
Atmospheric ground boundary layer z=0 *is* $C_0=b$,
The highest attitude z=z_t is $C_0=-az_t + b$

$$m\frac{d^2z}{dt^2} + C_0\frac{dz}{dt} + (C_0\eta + \alpha)z = C_0 V_{z0} - \beta$$

$$m\frac{d^2x}{dt^2} + C_0\frac{dx}{dt} = C_0(\varepsilon z + V_{x0})$$

Initial condition is *t=0* $\quad x=z=0$, $\quad dx/dt=V_{x0}$, $dz/dt=V_{z0}$
It solves differential equations as follows. 〔5〕
Characteristic equation;$m\lambda^2 + C_0\lambda + (C_0\eta + \alpha) = 0$

The root $\quad \lambda_{1,2} = [\ -C_0 \pm \sqrt{C_0{}^2 - 4m(C_0\eta + \alpha)}\ ]/2m$ ・

$$z = Ae^{\lambda 1\cdot t} + Be^{\lambda 2\cdot t} + \frac{C_0 V_{z0} - \beta}{C_0\eta + \alpha}$$

Fig.4 Wind velocity distribution by altitude 〔4〕

$$x = m\varepsilon\,(e^{-C_0/m\cdot t} - 1)\,[\ \frac{A}{m\lambda_1 + C_0} + \frac{B}{m\lambda_2 + C_0} + \frac{V_{z0} - \beta/C_0}{C_0\eta + \alpha}\ ]$$

$$+ C_0\varepsilon\,[\ \frac{A(e^{\lambda 1\cdot t} - 1)}{\lambda_1(m\lambda_1 + C_0)} + \frac{B(e^{\lambda 2\cdot t} - 1)}{\lambda_2(m\lambda_2 + C_0)}\ ]\ + t\,[\ \frac{C_0 V_{z0} - \beta}{C_0\eta + \alpha}\varepsilon + V_{x0}\ ]$$

here $\quad A = \dfrac{(C_0\eta + C_0\lambda_2 + \alpha)V_{z0} - \lambda_2\beta}{(\lambda_1 - \lambda_2)(C_0\eta + \alpha)}$, $\quad B = \dfrac{(C_0\eta + C_0\lambda_1 + \alpha)V_{z0} - \lambda_1\beta}{(\lambda_2 - \lambda_1)(C_0\eta + \alpha)}$
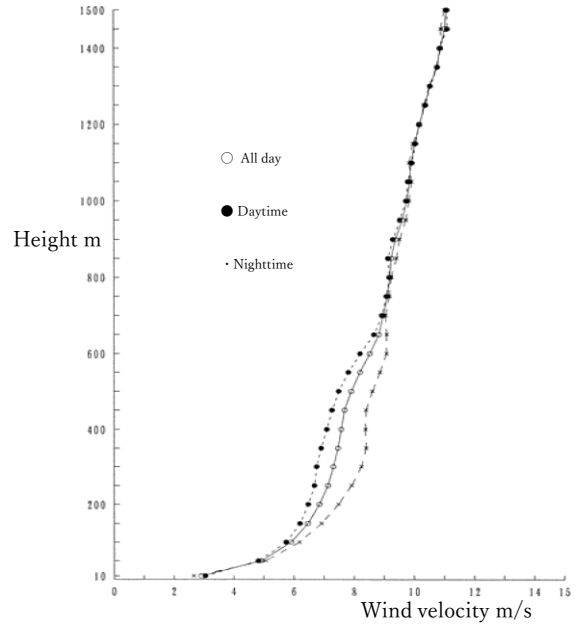
1.4. Correction by the air viscosity coefficient

The viscosity coefficient $C(z)$ of air was set to constant C_0 so that the differential equation could be solved. If the solutions in coefficient $C(0)$ are $z_2(t)$ and $x_2(t)$ in the viscosity at $z = 0$ at 100 m above ground, the solutions in the viscosity coefficient $C(z_t)$ at $z=z_t$ are $z_1(t)$ and $x_1(t)$, and the solution in any z can be approximated according to the interpolation equation as follows.

$$z(t)=(z_2-z_1)z(t)/z_t\ +z_1$$
$$\therefore\ \ z(t)=z_1\cdot z_t/\ (z_1-z_2+z_t\ )\qquad x(t)=x_1+\ (x_2-x_1)\cdot z(t)/z_t$$

The trial results of $[z_1(t), x_1(t)]$ and $[z_2(t), x_2(t)]$ and $[z(t), x(t)]$ are almost the same as shown in Table 1. And any may be adopted practically.

However, according to the numerical calculation example in Table 1, it takes about 4 hours for the radon cloud to reach an altitude of 1,000 m or more. Considering the natural diffusion of airborne radon concentration and scattering due to air flow turbulence over this long time, it is likely that almost horizontal cloud strips cannot be recognized. But it generates the vertical cloud near the earth face.

Table 1 Stream coordinates due to differences in air viscosity resistance

Time	Calculation at viscous $C(z_t)$ the top of the cloud		Calculation at viscous $C(0)$ the boundary layers		Practical value by interpolation equation	
(h)	x_2 (m)	z_2 (m)	x_1 (m)	z_1 (m)	x (m)	z (m)
0.0	0.0	0.0	0.0	0.0	0.0	0.0
1.0	24,115.0	377.3	24,117.7	377.7	24,117.2	377.6
2.0	52,581.8	679.7	52,591.0	680.3	52,587.7	680.1
3.0	84,536.0	922.0	84,554.2	922.8	84,545.4	922.4
4.0	119,285.3	1,116.2	119,313.4	1,117.0	119,296.9	1,116.6
5.0	156,274.5	1,271.9	156,312.8	1,272.7	156,287.1	1,272.2
6.0	195,058.7	1,396.6	195,107.1	1,397.4	195,071.5	1,396.8
7.0	235,281.6	1,496.6	235,339.5	1,497.3	235,293.9	1,496.7
8.0	276,657.4	1,576.7	276,724.2	1,577.4	276,668.8	1,576.8
9.0	318,957.2	1,640.9	319,032.0	1,641.5	318,967.4	1,641.0
10.0	361,997.5	1,692.4	362,079.4	1,692.9	362,006.4	1,692.4
12.0	449,740.5	1,766.6	449,834.4	1,767.0	449,747.1	1,766.7
13.3	509,132.3	1,800.7	509,232.4	1,801.1	509,137.5	1,800.7
48.0	2,099,026.4	1,900.0	2,099,152.5	1,900.0	2,099,026.4	1,900.0

1.5. Forms of ionization particles

The mass of m ionization particles near condensation nuclei, which is a cloud grain, is considered in three forms depending on the behavior of radon, and the streamlines of each are numerically compared, but as a result of numerical calculations, (1) (2) and (3) are the same in four effective digits. This is for a certain reason that ionization particles including radon are moving with the wind.

(1) The moisture particles gathered around ionization air and water move ... Density is 1000kg/m³ , no different from ordinary water

(2) The particles of ionization water vapor dissolved in radon gas move ... Radon's water solubility is 0.22ml/ml [6]. The density 1002kg/m³ of dissolved water is 0.2% heavier than water

(3) The radon gas particles move while ionizing the surroundings ... Radon gas density is 9.7 kg/m³ [6]

1. 6. Approximation calculation of radon gas sources

The streamline is a multiplier curve through the origin of the radon source as shown in Fig. 1 and approximates $z = z_t(1 - e^{-kx})$ simple exponential function.　By measuring the position differences (Δx, Δz) of the three places in the cloud strip, the distance to the origin x_1 can be approximated.

$$\frac{z_{31}}{z_{21}} = \frac{z_3 - z_1}{z_2 - z_1} = \frac{1 - e^{-kx_{31}}}{1 - e^{-kx_{21}}} \qquad , \qquad \frac{x_{31}}{x_{21}} = \frac{x_3 - x_1}{x_2 - x_1} = \frac{\log(z_t - z_1) - \log(z_t - z_3)}{\log(z_t - z_1) - \log(z_t - z_2)}$$

The unknown factors are k, z_t and they can be solved as follow that while k and z_t are slightly changing until the difference between both sides of the equation is 0.

$z_1 = z_t(1 - e^{-kx_1})$ From this, the distance to origin　$x_1 = -\frac{1}{k} \log(1 - z_1/z_t)$

Table 2 Data for exponential approximation by 3-point measurement

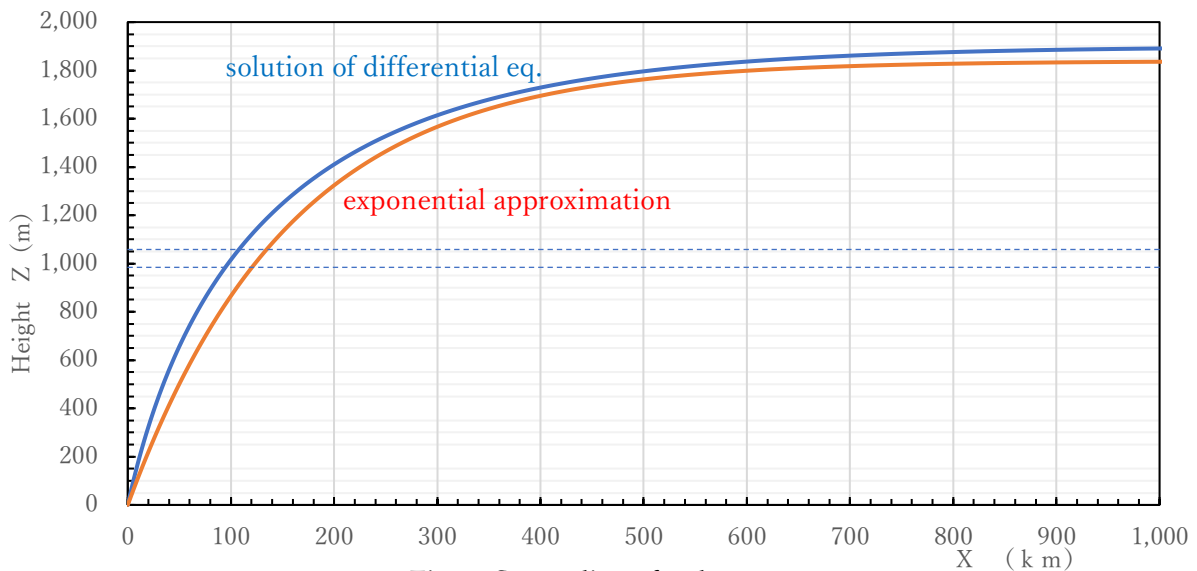|	Time (h)	x　(m)	z　(m)	
				$z = z_t(1 - e^{-kx})$
	5.67	181,968	1,358.3	Calculation of z_t result 1,839.0
	5.83	188,499	1,377.9	
	6.00	195,072	1,396.8	Calculation of k result 6.364x10⁻⁶
①	6.17	201,684	1,415.1	
②	6.33	208,335	1,432.6	Calculation of x_1 result 230,572
③	6.50	215,022	1,449.5	（Errors of x_1 ～15% in ① ）
	6.67	221,746	1,465.9	

Fig. 5 Streamline of radon

5

1. 7.　Behavior without horizontal wind velocity

If the horizontal wind velocity is $V_x(z) = \varepsilon z + V_{x0} = 0$, it is $\varepsilon = V_{x0} = 0$. As a result of **3.** x = 0 it is an upright cloud. However, the microscopic electric field effect of Q' by contact friction is verified here. Since there is no factor that determines the x.y axis, Newton's equation of motion is as follows in the polar coordinate display:

r direction　$m\left[\dfrac{d^2r}{dt^2} - r\left(\cancel{\dfrac{d\theta}{dt}}\right)^2\right] + C(z)\left(\dfrac{dr}{dt} - \cancel{V_r}\right) + Q' \cdot \dfrac{\partial\sqrt{}}{\partial r} = 0$

z direction　$m\dfrac{d^2z}{dt^2} + C(z)\left(\dfrac{dz}{dt} - V_z\right) + G(z)g + Q' \cdot \dfrac{\partial\sqrt{}}{\partial z} = 0$

Since it is $\ell_o \gg r,z$ near the origin, it is $\dfrac{\partial\sqrt{}}{\partial r} = \dfrac{\partial}{\partial r}\left[\dfrac{-1}{\sqrt{r^2+(z+d_o)^2}}\right] \fallingdotseq \dfrac{r}{d^3}$, Q' is neglected in derection z.

$$m\frac{d^2r}{dt^2} + C_0\frac{dr}{dt} + \frac{Q'r}{d_o{}^3} = 0$$

This differential equation is solved under the initial conditions $r=r_0$ and $dr/dt = 0$ at t=0.

$$z = Ae^{\lambda_1 \cdot t} + Be^{\lambda_2 \cdot t} + \frac{C_0 V_{z0} - \beta}{C_0\eta + \alpha}$$

$$r = \frac{r_0}{\lambda_4 - \lambda_3}(\lambda_4 e^{\lambda_3 \cdot t} - \lambda_3 e^{\lambda_4 \cdot t}) \quad \fallingdotseq r_0$$

$$\lambda_{3,4} = [-C_0 \pm \sqrt{C_0{}^2 - 4mQ'/d_o{}^3}]/2m \ t$$

Since dr/dt >0, r is an increase function. but as a result of the numerical calculation, it rises upright with little change in diameter in the vicinity of the origin. If the charge and radon gas do not happen at the same time, it is Q'= 0 . so that $\lambda_3 = 0$, $r=r_0$ constant.

Upright clouds taken directly above Akashi-Kaikyo Bridge in the epicenter vicinity one week before the Hyogo South Earthquake, occurred on the evening of Jan.9. (Courtesy of Mis.T. Sugie, NEWS Post Seven)

Photo 1　Upright cloud　〔7〕

1. 8.　Result of cloud strip

These calculation formulas are limited that the density, number of viscosity coefficients, and vertical wind velocity of air decrease almost linearly with altitude z, and the horizontal wind velocity increases, and it is established in the range of altitude (z < 10 km).

Furthermore, the water solubility of the inert radon gas is 0.22 ml/ml, which is about 1/3 times that of CO_2 and about 1000 times that of air. In this way, radon is easily soluble in water, so if the radon source is

in a sea area, radon is absorbed by seawater, and a single cloud does not occur. Only when the source of radon is near on land, does a single-article cloud seem to appear.

The radon concentration in the atmosphere is highly seasonally dependent as shown in Fig. 1. It is low in summer when the amount of moisture in the atmosphere is high, and it is high in winter when the moisture content of the atmosphere is low. This is probably due to the amount of water dissolved in radon gas and the water films.

Radon rises almost vertically because the weather is calm and mostly windless during the morning and evening calm hours. The cloud visually trails like the smoke of stick incense from a Buddhist altar.

(Gassho, pray for those who died in the earthquake)

Conditions under which these unique clouds are observed;

(1) Terrestrial epicenter where radon is not dissolved in seawater   (2) Neither rainy nor cloudy weather

(3) Daytime when clouds are visible   (4) Stable wind direction and wind speed without radon scattering

(5) Humidity and temperature at which core condensation clouds is likely to occur

Due to the cloud trajectory, the Coulomb force is very small compared to the wind force, the approach of the cloud to the epicenter is also less than a few percent, and the radon streamline also has many observation constraints, so it is not considered to be an appropriate method for grasping the precursors of earthquakes. It is necessary to search for the precursor elements that can be observed constantly anytime and have large changes clearly and are also superior to the ground potential VAN method.

2．Electric Field Measurement

2．1 Calculation of the epicenter by the electric field of the electric dipole

Although the electric field vector, which is a background of the earth current, is refracted in terms of different dielectric constants, (appendix 2) it has reached the electric field observation point from the epicenter.

Since the charge of the dipole is temporarily generated underground by triboelectric charging, if the magnitude of the electric field synthesis vector can be measured at 7 points, the epicenter is numerically calculable with computer.

Photo 2: Electrostatic field sensor assembly kit devised by Osaka University laboratory

The equipment of the "electrostatic field sensor" (Photo 2) can be accurately calibrated by the 0 electric field in the electrostatic shielding box or the reference electric field in the parallel metal plate with voltage and the electric field disturbance of the air layer such as thunderclouds, wind and rain can be blocked with a metal plate lid.

The dielectric constants ε_r vary depending on the geological formation and geology of each region through which the line of electric force pass, but they are the same here. Assuming that the position of the dipole charge $\pm Q$ is $(x_a, y_a, z_a),(x_b, y_b, z_b)$, the coordinates of the observer point i are (x_i, y_i, z_i) i = 1, 2, 3, ...7, and the observed field value is Ei, the potential V and the electric field E are as follows.

$$V_i = \frac{Q}{4\pi\varepsilon_o\varepsilon_r}\cdot\left[\frac{+1}{\sqrt{(x_i-x_a)^2+(y_i-y_a)^2+(z_i-z_a)^2}}+\frac{-1}{\sqrt{(x_i-x_b)^2+(y_i-y_b)^2+(z_i-z_b)^2}}\right]$$

$$E_{xi} = -\frac{\partial V_i}{\partial x_i} = \frac{Q}{4\pi\varepsilon_o\varepsilon_r}\cdot\left[\frac{(x_i - x_a)}{[(x_i - x_a)^2 + (y_i - y_a)^2 + (z_i - z_a)^2]^{3/2}} - \frac{(x_i - x_b)}{[(x_i - x_b)^2 + (y_i - y_b)^2 + (z_i - z_b)^2]^{3/2}}\right]$$

$$E_{yi} = -\frac{\partial V_i}{\partial y_i} = \frac{Q}{4\pi\varepsilon_o\varepsilon_r}\cdot\left[\frac{(y_i - y_a)}{[(x_i - x_a)^2 + (y_i - y_a)^2 + (z_i - z_a)^2]^{3/2}} - \frac{(y_i - y_b)}{[(x_i - x_b)^2 + (y_i - y_b)^2 + (z_i - z_b)^2]^{3/2}}\right]$$

$$E_{zi} = -\frac{\partial V_i}{\partial z_i} = \frac{Q}{4\pi\varepsilon_o\varepsilon_r}\cdot\left[\frac{(z_i - z_a)}{[(x_i - x_a)^2 + (y_i - y_a)^2 + (z_i - z_a)^2]^{3/2}} - \frac{(z_i - z_b)}{[(x_i - x_b)^2 + (y_i - y_b)^2 + (z_i - z_b)^2]^{3/2}}\right]$$

$$E_i^2 = E_{xi}^2 + E_{yi}^2 + E_{zi}^2$$

Since there are seven unknowns: (x_a, y_a, z_a), (x_b, y_b, z_b) ,$Q/4\pi\varepsilon_o\varepsilon_r$, it can be solved numerically by Ei. measurement at seven points. Since the surface crust is not an insulator but a conductor with resistance, and the charge moves gradually, the calculation result is $z_b = 0$ it is also conceivable. When the charge dissipates (x_b, y_b, z_b) can be far-reaching.

〔Numerical Solution Method〕

$E_i\,(x_i, y_i, z_i),\ E_0$; measured values、 $\quad E_i\,(x_a, y_a, z_a, x_b, y_b, z_b, x_i, y_i, z_i)$; calculated values

$$D(x_a, y_a, z_a, x_b, y_b, z_b) = \Sigma_{i=1,2,\cdots 7}\left[\,E_i^2(x_a, y_a, z_a, x_b, y_b, z_b, x_i, y_i, z_i)/E_0^2 - E_i^2(x_i, y_i, z_i)/E_0^2\,\right]^2$$

$(x_a, y_a, z_a, x_b, y_b, z_b)$ vary. When $D(x_a, y_a, z_a, x_b, y_b, z_b)$ is minimum(0), $x_a, y_a, z_a, x_b, y_b, z_b$ is the solution.

2.2. Example of numerical calculation of electric field

In order to understand qualitative trends in numerical calculation of the charge position (x_a, y_a, z_a) (x_b, y_b, z_b), when the charge position $\times$ is varied as shown in Fig. 6, the square of the electric field strength ratio $(E_i/E_0)^2$ at the observation point o(x_i, y_i, z_i) are shown in Table 3 as examples of calculation.
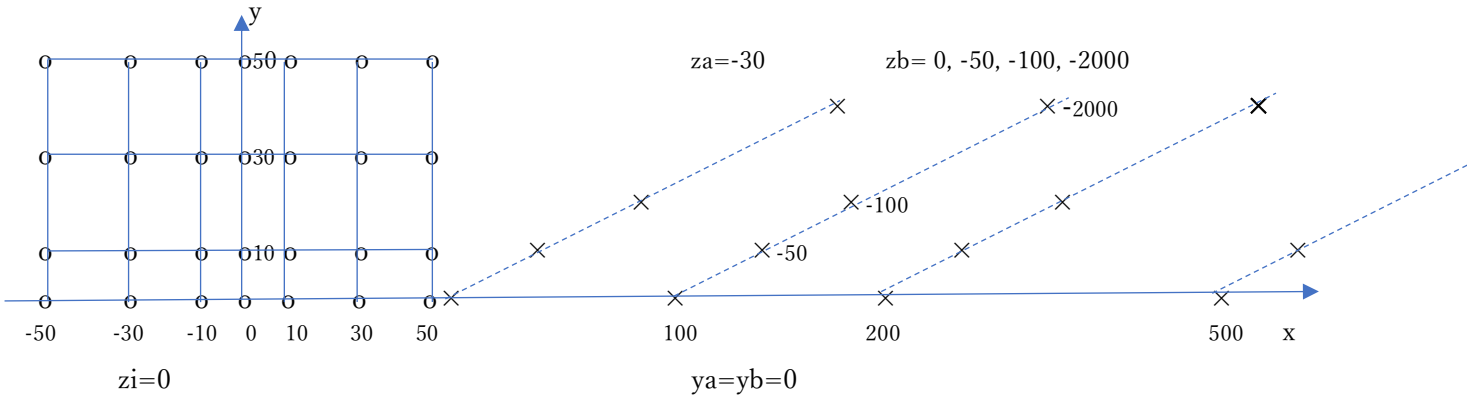
Fig.6 Position of charge and observation

2.3. Result of electric field method

Since simultaneous measurement at more than 7 points is necessary for the electric field method, the development and expansion of the observation network is awaited in the future. A lot of observation data must be accumulated and noise removal methods and the accuracy of epicenter prediction must be verified.

In addition, the intersection of the maximum electrostatic field orientation of the two observation points by the compass electrostatic field can be inferred to be a very rough epicenter.

Earthquake prediction seeks the following: When, where, and what size.

8

Table 3-1 Electric field ratio (Ei/Eo)^2 of observe point (xi, yi, 0)

dipole position	yi \ xi	-50	-30	-10	0	10	30	50
xa=xb=50	50	0.01	0.03	0.08	0.14	0.25	0.66	1.00
ya=yb=0	30	0.01	0.05	0.19	0.42	1.00	5.83	14.98
za=-30	10	0.02	0.07	0.33	0.90	2.86	62.64	2116
zb=0	0	0.02	0.07	0.36	1.00	3.37	105.23	100000
xa=xb=100	50	0.07	0.14	0.33	0.52	0.84	2.41	7.50
ya=yb=0	30	0.08	0.18	0.46	0.78	1.36	4.89	22.50
za=-30	10	0.09	0.21	0.56	0.97	1.79	7.50	47.67
zb=0	0	0.09	0.21	0.57	1.00	1.85	7.95	53.14
xa=xb=200	50	0.23	0.38	0.63	0.83	1.11	2.06	4.06
ya=yb=0	30	0.25	0.41	0.70	0.94	1.26	2.40	4.94
za=-30	10	0.26	0.43	0.74	0.99	1.35	2.61	5.47
zb=0	0	0.26	0.43	0.75	1.00	1.36	2.63	5.55
xa=xb=500	50	0.55	0.69	0.86	0.97	1.09	1.40	1.81
ya=yb=0	30	0.56	0.70	0.88	0.99	1.12	1.43	1.86
za=-30	10	0.56	0.70	0.89	1.00	1.13	1.45	1.88
zb=0	0	0.56	0.71	0.89	1.00	1.13	1.45	1.88

Electric field ratio (Ei/Eo)^2 of observe point (xi, yi, 0)
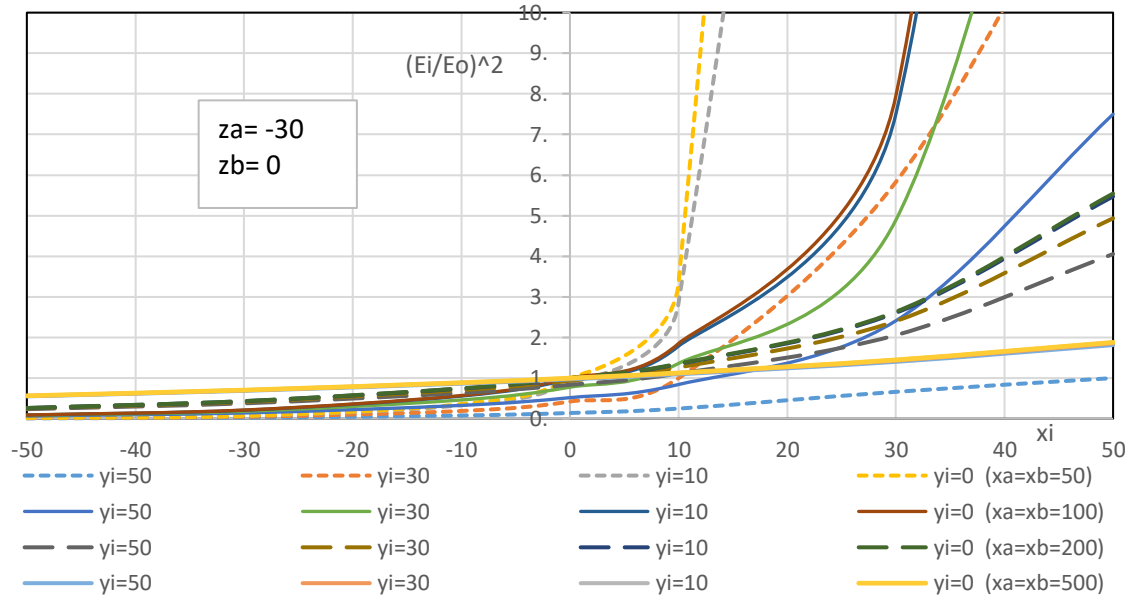
za= -30
zb= 0

Table 3-2 Electric field ratio (Ei/Eo)^2 of observe point (xi, yi, 0)

dipole position	yi \ xi	-50	-30	-10	0	10	30	50
xa=xb=50	50	0.02	0.04	0.11	0.19	0.31	0.72	1.00
ya=yb=0	30	0.02	0.07	0.25	0.49	1.00	3.57	6.31
za=-30	10	0.03	0.09	0.40	0.92	2.20	12.66	31.09
zb=-50	0	0.03	0.10	0.43	1.00	2.47	15.48	40.88
xa=xb=100	50	0.07	0.15	0.34	0.53	0.85	2.31	6.59
ya=yb=0	30	0.09	0.19	0.47	0.78	1.35	4.47	17.24
za=-30	10	0.09	0.22	0.57	0.97	1.74	6.59	31.97
zb=-50	0	0.10	0.22	0.58	1.00	1.80	6.95	34.85
xa=xb=200	50	0.23	0.38	0.63	0.83	1.11	2.05	4.03
ya=yb=0	30	0.25	0.41	0.70	0.94	1.26	2.40	4.90
za=-30	10	0.26	0.43	0.74	0.99	1.35	2.60	5.43
zb=-50	0	0.26	0.43	0.75	1.00	1.36	2.63	5.50
xa=xb=500	50	0.55	0.69	0.86	0.97	1.09	1.40	1.81
ya=yb=0	30	0.56	0.70	0.88	0.99	1.12	1.43	1.86
za=-30	10	0.56	0.70	0.89	1.00	1.13	1.45	1.88
zb=-50	0	0.56	0.71	0.89	1.00	1.13	1.45	1.88

Electric field ratio (Ei/Eo)^2 of observe point (xi, yi, 0)

za= -30
zb= -50
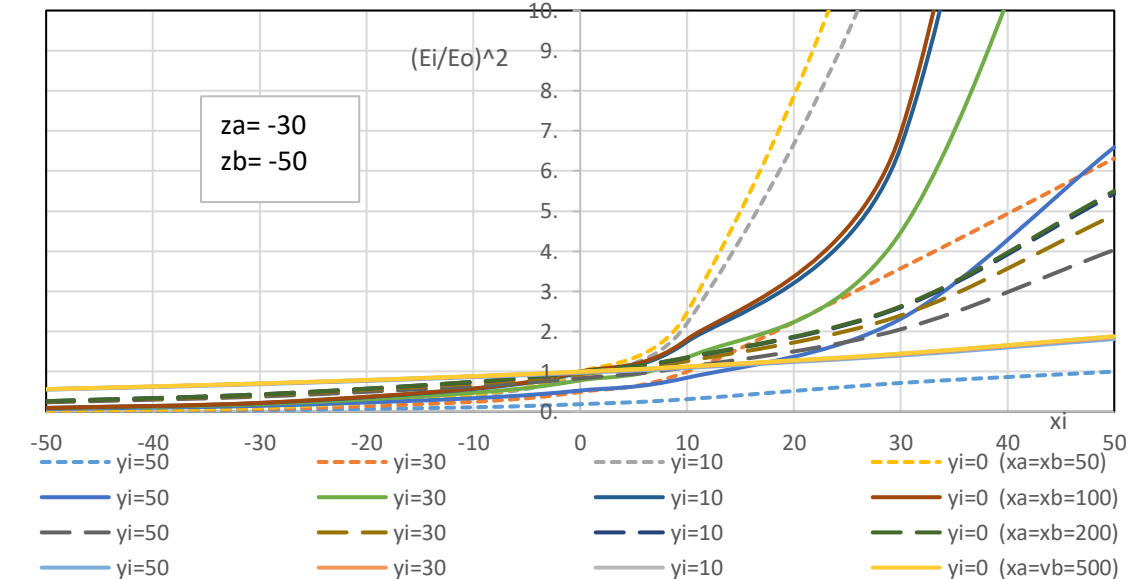
Table 3-3 Electric field ratio (Ei/Eo)^2 of observe point (xi, yi, 0)

dipole position	yi \ xi	-50	-30	-10	0	10	30	50
xa=xb=50	50	0.03	0.07	0.17	0.26	0.40	0.77	1.00
ya=yb=0	30	0.04	0.11	0.33	0.57	1.00	2.73	4.27
za=-30	10	0.05	0.15	0.48	0.93	1.86	7.43	15.35
zb=-100	0	0.05	0.15	0.51	1.00	2.04	8.72	19.22
xa=xb=100	50	0.09	0.18	0.38	0.57	0.87	2.05	4.91
ya=yb=0	30	0.11	0.23	0.52	0.81	1.29	3.57	10.70
za=-30	10	0.12	0.26	0.61	0.98	1.62	4.91	17.50
zb=-100	0	0.12	0.26	0.62	1.00	1.66	5.13	18.74
xa=xb=200	50	0.25	0.39	0.64	0.84	1.11	1.99	3.76
ya=yb=0	30	0.26	0.43	0.71	0.94	1.25	2.30	4.52
za=-30	10	0.27	0.44	0.75	0.99	1.33	2.49	4.97
zb=-100	0	0.28	0.45	0.76	1.00	1.34	2.51	5.03
xa=xb=500	50	0.55	0.69	0.86	0.97	1.09	1.40	1.81
ya=yb=0	30	0.56	0.70	0.88	0.99	1.12	1.43	1.85
za=-30	10	0.57	0.71	0.89	1.00	1.13	1.44	1.87
zb=-100	0	0.57	0.71	0.89	1.00	1.13	1.45	1.87

Electric field ratio (Ei/Eo)^2 of observe point (xi, yi, 0)

za= -30
zb= -100

(Ei/Eo)^2

yi=50 / yi=30 / yi=10 / yi=0 (xa=xb=50)
yi=50 / yi=30 / yi=10 / yi=0 (xa=xb=100)
yi=50 / yi=30 / yi=10 / yi=0 (xa=xb=200)
yi=50 / yi=30 / yi=10 / yi=0 (xa=xb=500)
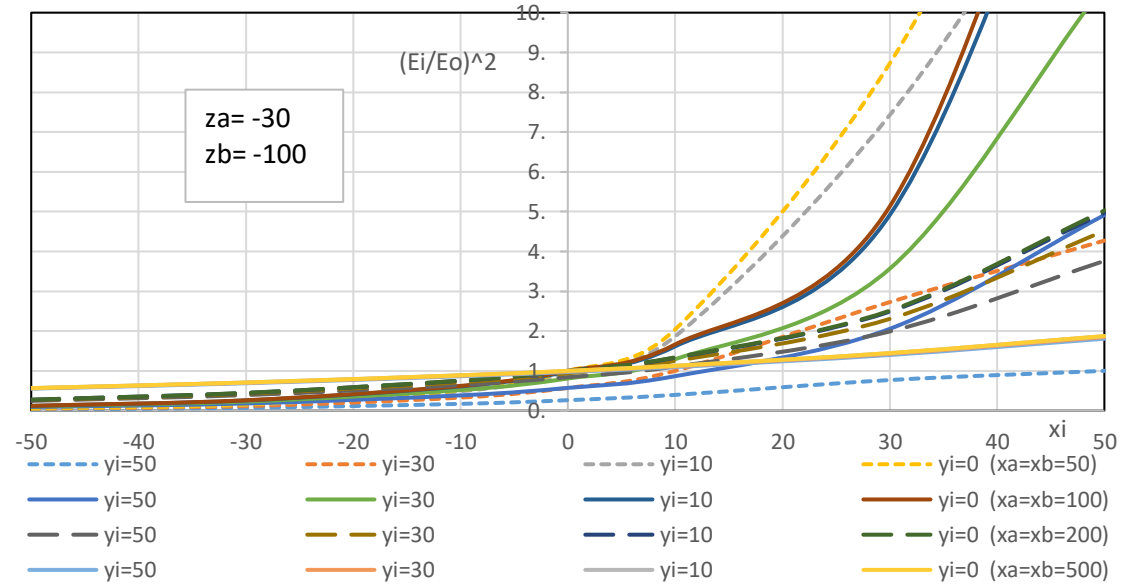
Table 3-4 Electric field ratio (Ei/Eo)^2 of observe point (xi, yi, 0)

dipole position	yi \ xi	-50	-30	-10	0	10	30	50
xa=xb=50	50	0.06	0.12	0.24	0.33	0.46	0.80	1.00
ya=yb=0	30	0.08	0.17	0.40	0.63	1.00	2.39	3.57
za=-30	10	0.10	0.21	0.55	0.94	1.71	5.90	11.57
zb=-2000	0	0.10	0.22	0.57	1.00	1.85	6.84	14.28
xa=xb=100	50	0.18	0.29	0.49	0.66	0.90	1.73	3.42
ya=yb=0	30	0.20	0.34	0.61	0.85	1.21	2.65	6.43
za=-30	10	0.21	0.37	0.69	0.98	1.44	3.42	9.71
zb=-2000	0	0.22	0.37	0.70	1.00	1.47	3.53	10.29
xa=xb=200	50	0.38	0.53	0.74	0.89	1.07	1.60	2.50
ya=yb=0	30	0.40	0.56	0.79	0.96	1.16	1.78	2.84
za=-30	10	0.41	0.58	0.82	1.00	1.22	1.87	3.03
zb=-2000	0	0.42	0.58	0.83	1.00	1.22	1.89	3.06
xa=xb=500	50	0.67	0.77	0.90	0.98	1.06	1.26	1.49
ya=yb=0	30	0.67	0.78	0.92	0.99	1.08	1.27	1.52
za=-30	10	0.68	0.79	0.92	1.00	1.08	1.28	1.53
zb=-2000	0	0.68	0.79	0.92	1.00	1.09	1.29	1.53

Electric field ratio (Ei/Eo)^2 of observe point (xi, yi, 0)

za= -30
zb= -2000

(Ei/Eo)^2

yi=50 / yi=30 / yi=10 / yi=0 (xa=xb=50)
yi=50 / yi=30 / yi=10 / yi=0 (xa=xb=100)
yi=50 / yi=30 / yi=10 / yi=0 (xa=xb=200)
yi=50 / yi=30 / yi=10 / yi=0 (xa=xb=500)
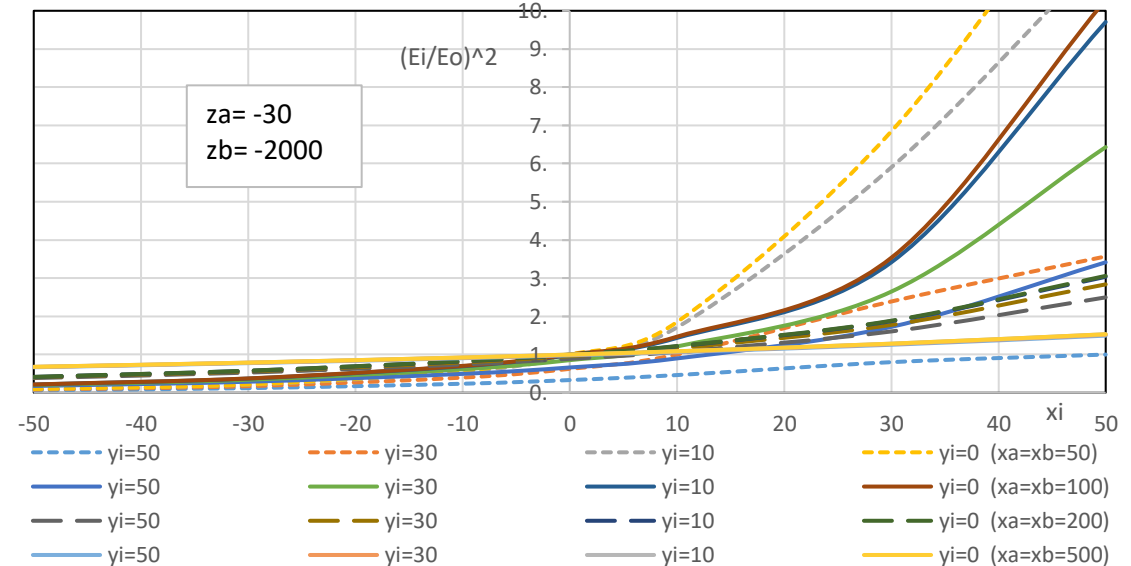
[Appendix 1]　Electric field of a point charge in a double-layer dielectric

If the contact surface of the two dielectrics is horizontal and a point charge is present in the lower layer, the electric field strength in the upper dielectric is calculated. Consider in the plane formed by the incident electric field vector $\mathbf{E_1}$ passing through the origin and the refracted electric field vector $\mathbf{E_2}$.

Using the position of the point charge Q as the coordinate origin,
the horizontal contact plane is the x-y plane.
the dielectric constant of the lower/upper layer dielectric is $\varepsilon_1 / \varepsilon_2$,
the angle of incidence/refraction of the electric field at the contact surface is θ_1 / θ_2,
the distance from the origin to the horizontal contact surface is r_1、
the distance to an arbitrary point P of the refracted field vector is r,
the height coordinate of an arbitrary point P from the origin is z,
the height of the horizontal contact plane from the origin is z_B,

Fig.7 coordinate sign
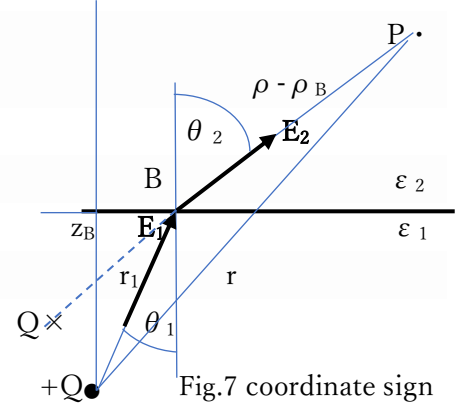
Depending on the boundary conditions of the dielectric, the tangential component of the electric field is continuous　$(\mathbf{E_1}-\mathbf{E_2}) \cdot \mathbf{t} = 0$　　$E_{1t} = E_{2t}$

The normal component is discontinuous　$(\varepsilon_1 \mathbf{E_1} - \varepsilon_2 \mathbf{E_2}) \cdot \mathbf{n} = 0$　　$\varepsilon_1 E_{1n} = \varepsilon_2 E_{2n}$.

The relationship between the angle of incidence and the angle of refraction is $\tan\theta_1 / \tan\theta_2 = \varepsilon_1 / \varepsilon_2$ and geometrically $\tan\theta_1 = \sqrt{r_1^2 - z_B^2}/z_B$.

Therefore, the electric field strength at the refractive point B is as follow.

$$|\boldsymbol{E_1}|_B = \frac{Q}{4\pi\varepsilon_1 r_1^2} \qquad |\boldsymbol{E_2}|_B = \frac{Q\varepsilon_2(r_1^2 - z_B^2)}{4\pi\varepsilon_1 r_1^3\sqrt{\varepsilon_1^2 z_B^2 + \varepsilon_2^2(r_1^2 - z_B^2)}}$$

The electric field vector $\mathbf{E_1}$ of the point charge is evenly radiated in all directions. While the field strength is attenuated at distance, the electric field vector $\mathbf{E_1}$ moves straight and hits the boundary surface, changing its size and direction. The electric field vector $\mathbf{E_2}$ that has shifted to the new dielectric moves straight in the new direction while attenuating distance. That is, in dielectric 2, there is an imaginary origin at a certain place in the direction opposite to the direction of travel of $\mathbf{E_2}$. (Same idea as refraction by optical mirrors and lenses). If the distance from the imaginary origin to the refractive point B is ρ_B, and the distance to the arbitrary point P is ρ, then

$$|\boldsymbol{E_2}|_B = Q/4\pi\varepsilon_2\rho_B^2 , \qquad |\boldsymbol{E_2}| = Q/4\pi\varepsilon_2\rho^2$$

Geometrically, it is $r^2 = (\rho - \rho_B)^2 + r_1^2 - 2(\rho - \rho_B)r_1 \cos(\pi + \theta_1 - \theta_2)$. If it solves this,

$$|\boldsymbol{E_2}| = \frac{Q}{4\pi\varepsilon_2 r^2} \cdot \cfrac{1}{\left[\sqrt{1 - \dfrac{(\varepsilon_1 - \varepsilon_2)^2 z_B^2(r_1^2 - z_B^2)}{r^2[\varepsilon_1^2 z_B^2 + \varepsilon_2^2(r_1^2 - z_B^2)]}} - \dfrac{\varepsilon_1 z_B^2 + \varepsilon_2(r_1^2 - z_B^2)}{r\sqrt{\varepsilon_1^2 z_B^2 + \varepsilon_2^2(r_1^2 - z_B^2)}} + \dfrac{r_1}{r}\sqrt{\dfrac{\varepsilon_1 r_1}{\sqrt{\varepsilon_1^2 z_B^2 + \varepsilon_2^2(r_1^2 - z_B^2)}}}\right]^{\wedge 2}}$$

So that, **the above equation is roughly $E = Q/4\pi\varepsilon_2 r^2$** , also

$$z = z_B + \left[\sqrt{r^2[\varepsilon_1^2 z_B^2 + \varepsilon_2^2(r_1^2 - z_B^2)] - (\varepsilon_1 - \varepsilon_2)^2 z_B^2(r_1^2 - z_B^2)} - \varepsilon_1 z_B^2 - \varepsilon_2(r_1^2 - z_B^2)\right] \times$$
$$\varepsilon_1 z_B /[\varepsilon_1^2 z_B^2 + \varepsilon_2^2(r_1^2 - z_B^2)]$$

[Appendix 2]　Values used for numerical calculation　　（unit system is m , kg , sec , Amp）

　fog diameter d $=1\times10^{-5}$　fog mass　m$= 5.236\times10^{-13}$

　wind velocity　　Vx$=3.57\times10^{-3}$ z $+ 6$　　Vz$= -6.15\times10^{-5}$ z $+0.12$

　cloud top altitude $z_t=$ cloud top2000-boundary layer100　　　epicenter depth $d_0=20,000/30,000$

　charge term Q'$=10^{-20}$

　viscous term C$=-3.77\times10^{-14}$ z $+1.70\times10^{-9}$

　gravity term G$=4.11\times10^{-18}$ z $+5.13\times10^{-12}$

　initial condition　t=0　x= z =0　　Vxo=6　Vzo=0.12

　radon collapse process(half-life)　　$^{226}_{88}$Ra(1600y)$\to$ $^{222}_{86}$Rn(3.8d)$\to$ $^{218}_{84}$Po(3.1m)$\to$ $^{214}_{82}$Pb$\Rightarrow$ $^{206}_{82}$Pb

References

[1] Observation of atmospheric radon concentration before the Hyogo South Earthquake,
　　National Institute of Radiological Sciences Leaflet, Tetsuo Ishikawa December 2018,
　　www.qst.go.jp/site/qms/1575.html

[2] Lecture of cloud chamber, Institute of Environmental Science and Technology, February 2007.
　　www.ies.or.jp/publicity_j/mini/2006-07.pdf

[3] www. Standard atmosphere - Calculation formula of air temperature, pressure, density, sound speed,
　　viscosity coefficient, and dynamic viscosity coefficient at each altitude

[4] Average wind speed vertical distribution by altitude www.city.nagoya.jp/.../48Jhyoka_shiryo_01_02.pdf

[5] Official View of Higher Mathematics Translated by Kawamura & Imoto, Asakura Shoten 2013

[6] Radon Physical and Chemical Information, ILO and WHO 2018,
　　www.ilo.org/dyn/icsc/showcard.display?p_lang=ja&p_card_id=1322&p_version=2

[7] "Earthquake clouds" witnessed in the Great Hanshin-Awaji Earthquake have "no scientific basis whatsoever"
　　Above in news.yahoo.co.jp/.../525a9287cf4ecb98402daf1488d4c.